



Original Article

A panel of miRNAs in serum extracellular vesicles serves as novel diagnostic biomarkers for MASLD

Moran Hu^{a,1}, Hai Huang^{a,b,1}, Meng Jia^{c,1}, Min Xu^d, Malin Chen^e, Junxiang Wu^b, Shouyong Gu^d, Hongwei Liang^{b,*}, Hongwen Zhou^{a,**}, Yingyun Gong^{a,***}

^a Department of Endocrinology and Metabolism, The First Affiliated Hospital of Nanjing Medical University, Jiangsu, China

^b Department of Emergency, Nanjing Drum Tower Hospital, School of Life Science and Technology, China Pharmaceutical University, Jiangsu, China

^c State Key Laboratory of Pharmaceutical Biotechnology, Department of Gastroenterology, Nanjing Drum Tower Hospital, The Affiliated Hospital of Nanjing Medical University, Nanjing University, Jiangsu, China

^d Institute of Geriatric Medicine, Jiangsu Province Geriatric Hospital, Nanjing, Jiangsu, China

^e The First Clinical College of Nanjing Medical University, Jiangsu, China

ARTICLE INFO

Keywords:

MASLD
Extracellular vesicles
WGA-coupled magnetic beads
miRNA

ABSTRACT

The rising global prevalence of metabolic dysfunction-associated steatotic liver disease (MASLD) poses a growing challenge to healthcare systems, stimulating substantial research efforts to develop reliable diagnostic methodologies. Emerging evidence highlights extracellular vesicles (EVs) as promising non-invasive biomarkers due to their roles in metabolic regulation and disease progression. This study investigated the diagnostic potential of serum EV-derived microRNAs (miRNAs) for MASLD detection and staging. We developed a novel diagnostic approach combining wheat germ agglutinin (WGA)-coupled magnetic beads for EV capture with RT-qPCR analysis, creating a streamlined two-step protocol that eliminates conventional purification requirements. MiR-574-3p, miR-542-3p, and miR-200a-3p in serum EVs were significantly elevated in patients with MASLD, indicating their potential as non-invasive biomarkers. Here, our established platform offers a clinically feasible solution for EVs isolation and quantitative miRNA analysis, presenting significant advantages in diagnostic efficiency and practical implementation.

Introduction

Metabolic dysfunction-associated steatotic liver disease (MASLD) affects one in four adults worldwide, currently has a prevalence rate of 25.2%, and is expected to rise to 33.5% by 2030 [1,2]. In China, the prevalence has grown from 23.8% in the early 21st century to 32.9% in 2018, with projections indicating a total of 315 million cases by 2030 [3]. This positions China as the country with the fastest-growing rate of MASLD. This condition is defined by the excessive accumulation of lipids within hepatocytes and has the potential to advance to more severe pathologies, including metabolic dysfunction-associated steatohepatitis, cirrhosis, and hepatocellular carcinoma [4]. Additionally,

MASLD is associated with chronic kidney disease, cardiovascular disease, and sleep apnea [1,4]. Early diagnosis is crucial for halting disease progression; however, current diagnostic methods like liver biopsy have their limitations [5]. Noninvasive assessment tools such as the fatty liver index and hepatic steatosis index serve as initial screening options, while imaging techniques like ultrasound and MRI offer more precise evaluations but are not widely accessible [5]. Therefore, it is critical to develop new diagnostic biomarkers for enhancing early detection and treatment of MASLD.

Exosomes are a kind of small extracellular vesicles (EVs) with approximately 100 nm in diameter [6]. They are released from various cell types and can be found in a variety of biological fluids [6]. Research

* Corresponding author. School of Life Science and Technology, China Pharmaceutical University, Nanjing, Jiangsu, 210009, China.

** Corresponding author. Department of Endocrinology and Metabolism, The First Affiliated Hospital of Nanjing Medical University, Nanjing, Jiangsu, 210029, China.

*** Corresponding author. Department of Endocrinology and Metabolism, The First Affiliated Hospital of Nanjing Medical University, Nanjing, Jiangsu, 210029, China.

E-mail addresses: hwliang@cpu.edu.cn (H. Liang), drhongwenzhou@njmu.edu.cn (H. Zhou), gongyingyun@njmu.edu.cn (Y. Gong).

¹ These authors contributed equally to this work.

has highlighted their essential roles in intercellular communication by microRNAs (miRNAs) and other non-coding RNAs [6,7]. MiRNAs, which are 20–25 nt small non-coding RNAs, could result in mRNA translation inhibition or degradation [8]. Recent studies have emphasized the significance of miRNAs in MASLD disease progression, owing to their capacity to regulate genes implicated in lipid metabolism, inflammation, fibrosis, and cell proliferation. In addition, the modulation of miRNAs through synthetic molecules emerges as a promising therapeutic strategy. Due to the protective effect of the membrane, exosomal miRNAs are resistant to degradation by ribonucleases and play a significant role in regulating cell growth, proliferation, and metabolism. These miRNAs are currently being explored as potential biomarkers for multiple kinds of disease, including MASLD [7,9].

However, the practical application of exosomal miRNAs as biomarkers has been limited due to the lack of straightforward capture and analysis methods. Conventional techniques for isolating and quantifying exosomal miRNAs tend to be time-consuming, labor-intensive, and costly, rendering them impractical for clinical settings. In prior studies, both we [10,11] and Boan Li et al. [12] developed a novel and efficient approach for capturing and analyzing EVs using wheat germ agglutinin (WGA)-coupled magnetic beads. We presented a straightforward and efficient approach for separating and precisely quantifying miRNAs within EVs derived from serum, utilizing WGA-coupled magnetic beads and reverse transcription quantitative polymerase chain reaction (RT-qPCR). Our findings indicate that miR-574-3p, miR-542-3p, and miR-200a-3p in serum EVs hold potential as promising diagnostic biomarkers for MASLD.

Material and methods

Study design and cohort information

The flowchart of the present study is depicted in [Fig. 1]. As shown in panel A, WGA-coupled magnetic beads were added to human serum samples, aiming to enrich EVs. RNA extraction was performed for unbiased small RNA sequencing or RT-qPCR validation. Two independent cohorts from the First Affiliated Hospital of Nanjing Medical University were included in the current study for discovery and validation. The first cohort recruited patients from 2019 Feb to 2022 Nov, and the second cohort recruited patients from 2023 Aug to 2024 Jan. Patients qualified with overweight or obesity (BMI ≥24 kg/m²) were subjected to evaluating metabolic health status. Written consents were obtained from those patients enrolled for clinical sample collection and routine follow-up. The inclusion criterion required confirmation of MASLD through

liver biopsy. The exclusion criteria included: 1) excess alcohol (men >30 g/day and women >20 g/day); 2) patients with other chronic liver diseases; 3) patients with decompensated liver cirrhosis; 4) individuals with other severe systemic diseases; and 5) pregnant women. Age- and gender-matched lean volunteers without MASLD (healthy control, HC) were enrolled as well. In detail, cohort 1-I (MASLD n = 9 and HC n = 9) set as the discovery subgroup and underwent EVs RNA sequencing, cohort 1-II (MASLD n = 72 and HC n = 30) served as internal validation using RT-qPCR, and the independent cohort 2 (MASLD n = 24 and HC n = 10) turned as another validation group using RT-qPCR as well. Clinical characteristics, including histopathological, demographic, and laboratory findings for both patients diagnosed with MASLD and healthy controls, were summarized in [Table 1] (cohort 1-II), [Table S1] (cohort 1-I), and [Table S2] (cohort 2). The study received approval from the Human Research Ethics Committee of the First Affiliated Hospital of Nanjing Medical University (2018-SR-069) and was conducted following the Declaration of Helsinki.

Clinical sample collection

To ensure EV integrity, serum samples were centrifuged within 4 h of collection. Firstly, blood samples were centrifuged at 300 g for 10 min, followed by 3000 g for another 10 min. Secondly, the supernatants were carefully transferred to new tubes and stored in an ultra-low-temperature freezer at −80 °C for further processing.

Separate EVs using WGA-coupled magnetic beads

EVs were separated using WGA-coupled magnetic beads as previously described [10,11]. To remove cellular debris, serum samples were first centrifuged for 20 min at 3000 g. Next, 1 mL of serum was incubated with 5 μL of WGA-coupled magnetic beads (C995Y30, Thomas Scientific) for 1 h at room temperature. Then, the EVs were separated by placing the tube on a magnet for 5 min and discarding the supernatants.

Table 1
Clinical characteristics of cohort 1-II.

| Characteristic | MASLD (n = 72) | HC (n = 30) | P value |
|------------------------------|----------------|---------------|---------|
| Age, median (IQR), years | 56 (44–64) | 57 (42–65) | – |
| Male, n (%) | 23 (31.9) | 10 (33.3) | – |
| BMI (kg/m ²) | 27.45 ± 4.72 | 20.82 ± 2.80 | <0.001 |
| ALT (U/L) | 77.84 ± 75.54 | 22.25 ± 23.43 | <0.001 |
| AST (U/L) | 49.67 ± 38.71 | 24.25 ± 11.56 | <0.001 |
| Fibrosis stage, n, 0/1/2/3/4 | 4/8/6/17/37 | | |

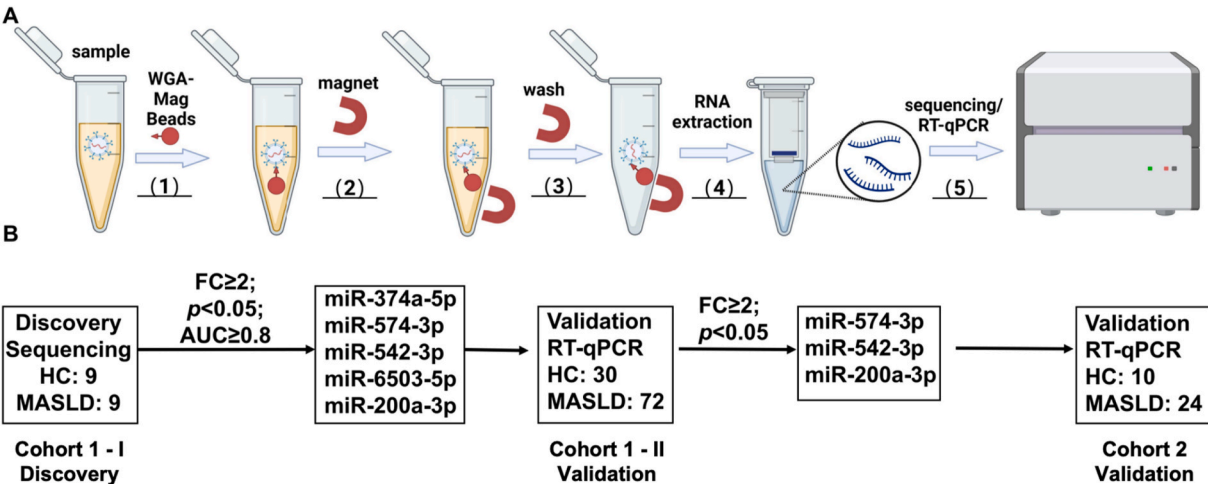


Fig. 1. Workflow for the investigation of the serum exosomal miRNAs. Abbreviations: HC: healthy control; MASLD: metabolic dysfunction-associated steatotic liver disease; FC: fold change; AUC: area under curve.

Finally, phosphate-buffered saline (PBS) was used to wash the EVs on the WGA-coupled magnetic beads.

EVs characterization

EVs were eluted by 500 mM N-acetyl-D-glucosamine elution buffer from WGA-coupled magnetic beads. Subsequently, the EVs were characterized by transmission electron microscopy (TEM), nanoparticle tracking analysis (NTA), and Western Blotting as previously reported [10,11]. In brief, a Hitachi 7500 TEM was applied to visualize the shape and size of EVs. EVs containing samples were prefixed with a solution supplemented with 5% bovine serum albumin and 2.5% glutaraldehyde, then postfixed with 2% osmium tetroxide, followed by routine dehydration, and embedding. Ultrathin sections ranging from 80 to 90 nm in thickness were ideal choices for further TEM analysis. NTA is an alternative method to analyze the size and concentration of EV particles based on the Nanosight NS300 system (Malvern, UK). The antibodies utilized for Western Blotting in this study included CD9 (20597-1-AP, Proteintech), TSG101 (28283-1-AP, Proteintech), CD63 (52090S, CST), ALIX (12422-1-AP, Proteintech), GM130 (11308-1-AP, Proteintech), and the horseradish peroxidase-conjugated secondary antibodies (ab205718, Abcam).

Small RNA sequencing & RT-qPCR

A total of 18 samples in cohort 1-I were prepared for small RNA sequencing. In addition, cohort 1-II and cohort 2 were used for validation, using RT-qPCR. TRIzol Reagent (Invitrogen, USA) was used to extract total RNA from EVs as manual. The OneDrop-2000 spectrophotometer (NanoDrop Technologies) was used to assay the quantity and purity of the extracted RNA. Small RNA sequencing was performed by BGI (Shenzhen, China), and the RT-qPCR for the selected miRNAs was carried out by the miRNA 1st Strand cDNA Synthesis Kit (Vazyme Biotech, China) and the miRNA Universal SYBR qPCR Master Mix (Vazyme Biotech, China). The primers for the miRNAs were obtained from Thermo Fisher Scientific (USA).

Statistical analysis

GraphPad Prism 9.0 was used to analyze the data and the p-value of less than 0.05 was considered statistically significant. Statistical analyses were performed using Student's t-tests and one-way ANOVA, followed by Tukey's test, while considering sample distribution and variance.

Results

WGA-coupled magnetic beads isolated EVs from serum

Previous studies have shown that EVs are abundant in glycoproteins and can bind to various lectins, including WGA [10,11]. An innovative, user-friendly, and highly efficient methodology for capturing EVs from serum and urine by WGA-coupled magnetic beads was developed [10,11]. In this study, the EVs in the serum of patients with MASLD and healthy volunteers was captured by WGA-coupled magnetic beads [Fig. 1]. Subsequently, TEM, NTA, and Western blotting was performed to characterize the isolated EVs. The EVs exhibited a bilayer membrane structure with about 100 nm diameter [Fig. 2A–B]. According to NTA analysis, the concentration and size of the EVs isolated by the WGA-coupled magnetic beads had no difference between MASLD and healthy controls [Figure S1]. Furthermore, western blotting indicated exosomal markers, including CD9, TSG101, ALIX, and CD63, presented in the exosomes, while the GM130, the marker for Golgi apparatus-derived membrane-bound vesicles, was not detected in the exosomes [Fig. 2C]. In conclusion, the EVs in the serum were successfully captured by WGA-coupled magnetic beads.

Small RNA sequencing of EVs in the serum

Exosomes in the serum of 9 healthy individuals and 9 patients with MASLD were captured by WGA-coupled magnetic beads and subsequently performed small RNA-sequencing. As the result shown in [Fig. 3A], miRNAs in serum EVs could clearly distinguish MASLD patients from HCs by principal component analysis. The volcano plot identified 19 dysregulated miRNAs, including 8 upregulated and 11 downregulated [Fig. 3B]. The heatmap also demonstrated a consistent trend of differentially expressed miRNAs in the 9 healthy individuals and 9 patients with MASLD [Fig. 3C].

GO analysis and KEGG enrichment analysis of the functions of dysregulated miRNAs in the serum exosomes

The PANTHER database was employed to analyze the GO and KEGG pathways that are associated with the dysregulation of miRNAs. The miRNAs found to be upregulated in serum exosomes are primarily linked to the regulation of transcription from RNA polymerase II promoters and the biosynthesis of unsaturated fatty acids, among other functions [Fig. 4A]. In contrast, the downregulated miRNAs in serum exosomes are mainly associated with the regulation of transcription from RNA polymerase II promoters, the Hippo signaling pathway, and the TGF-beta signaling pathway, among others [Fig. 4B]. These findings indicate that the differentially expressed miRNAs in EVs may be involved in transcriptional regulation and the inflammatory response related to the

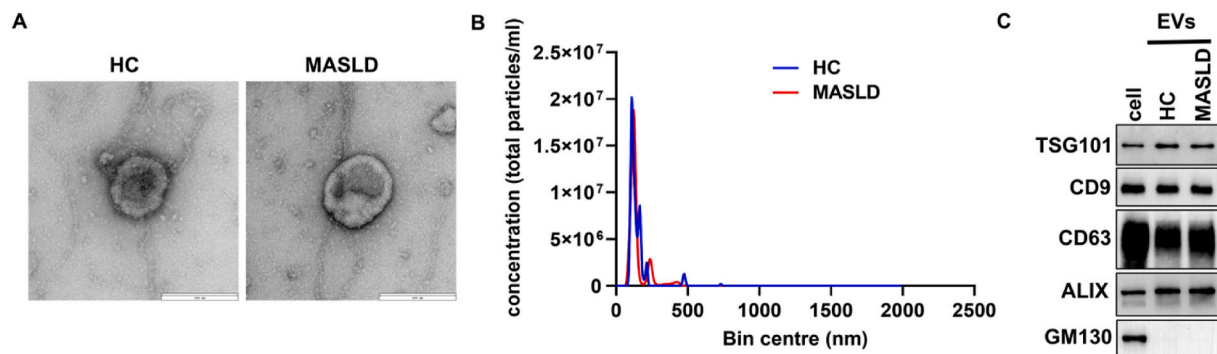


Fig. 2. Identification of EVs isolated by WGA-coupled magnetic beads. (A) TEM analysis of exosomes isolated by WGA-coupled magnetic beads. Scale bar 100 nm. (B) NTA quantification of exosomes isolated by WGA-coupled magnetic beads. (C) Western blotting analysis of exosomes (30 μ g) isolated by WGA-coupled magnetic beads and cell lysate (60 μ g). Data from three independent experiments.

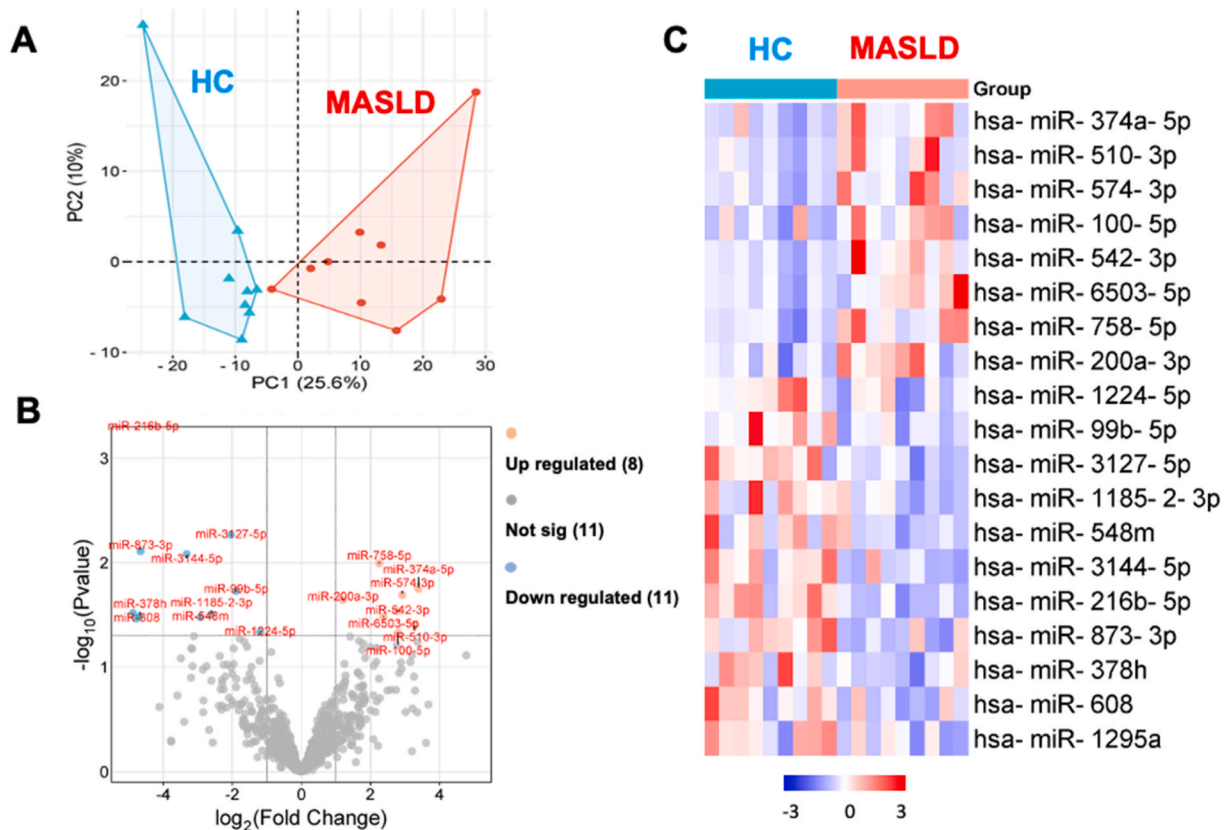


Fig. 3. Small RNA analysis of exosomes from MASLD patients and HC. (A) PCA analysis. (B) Volcanic plot analysis. (C) Heat map of exosome differential miRNAs. Blue represents decreased miRNAs; red represents increased miRNAs.

progression of MASLD.

Biomarker-validation phase of the miRNAs in the serum exosomes for MASLD

To evaluate the diagnostic potential of the 19 dysregulated miRNAs in serum exosomes for detecting MASLD through RNA sequencing, we conducted ROC curve analysis. As shown in [Table 2], the area under the curve (AUC) values for miR-374a-5p, miR-574-3p, miR-542-3p, miR-6503-5p, and miR-200a-3p exceeded 0.8, leading to their selection for further investigation. Subsequently, these five miRNAs were validated in a larger cohort consisting of 72 MASLD patients and 30 healthy volunteers using RT-qPCR [Fig. 1]. As depicted in [Fig. 5A], the expression levels of miR-574-3p, miR-542-3p, and miR-200a-3p were significantly upregulated in serum EVs derived from MASLD patients, in contrast to those from healthy volunteers. Conversely, no statistically significant variations were observed in the levels of miR-374a-5p and miR-6503-5p between the two groups, as illustrated in [Fig. 5A–E]. Furthermore, ROC curve analysis revealed that the expression levels of miR-574-3p, miR-542-3p, and miR-200a-3p in serum EVs effectively distinguished MASLD patients from healthy volunteers [Fig. 5F] and [Table 3]. Moreover, the combined model of the three miRNAs exhibited the highest discriminatory power in distinguishing MASLD patients from healthy individuals by the binary logistic regression analysis [Fig. 5F] and [Table 3].

To further validate the diagnostic effect of the miR-574-3p, miR-542-3p, and miR-200a-3p, the RT-qPCR was performed in another cohort [Table S2]. Consistent with the previous results, the expression levels of miR-574-3p, miR-542-3p, and miR-200a-3p were significantly upregulated in serum EVs derived from MASLD patients [Figures S2A–C], and the Area Under Curve (AUC) of the combined model of the three miRNAs by ROC curve analysis was 0.9672 [Figure S2D] with 91.67% sensitivity and 100% specificity [Figure S2E].

Analysis of miR-574-3p, miR-542-3p, and miR-200a-3p expression patterns in the serum exosomes based on the degree of fibrosis stage

We investigated the variations in serum exosomal miRNA concentrations among MASLD patients with differing degrees of disease severity. Elevated alanine aminotransferase (ALT) and aspartate aminotransferase (AST) levels are nonspecific indicators of hepatocellular damage. In nonalcoholic fatty liver disease (NAFLD) and nonalcoholic steatohepatitis (NASH), ALT and AST levels may be elevated two to four times above the upper limit of normal [13]. However, our study found that the expression levels of miR-574-3p, miR-542-3p, and miR-200a-3p in exosomes did not correlate with the ALT and AST concentrations in the blood [Figure S3]. In terms of fibrosis severity, miR-542-3p was significantly increased in MASLD patients with fibrosis stage 2 or higher compared to those with fibrosis stage less than 2, and this trend continued with a significant increase in miR-542-3p and miR-200a-3p in patients with fibrosis stage 3 or higher compared to those with fibrosis stage less than 3, whereas miR-574-3p remained unchanged [Fig. 6A–C].

Discussion

MASLD, the most common liver disease worldwide, presents significant public health challenges due to its links to hepatitis, cirrhosis, and liver cancer [1,2]. The prevalence of MASLD is steadily rising within our population, with approximately 4% of new cases being reported annually [2]. Notably, regional differences in prevalence rates reflect lifestyle variations; economically developed eastern and southern regions exhibit higher rates than central and western areas [2]. Over the past two decades, China's economic growth and changes in lifestyle have led to a marked rise in MASLD cases [3]. Early detection is crucial for effective intervention; however, there is a significant lack of diagnostic tools for

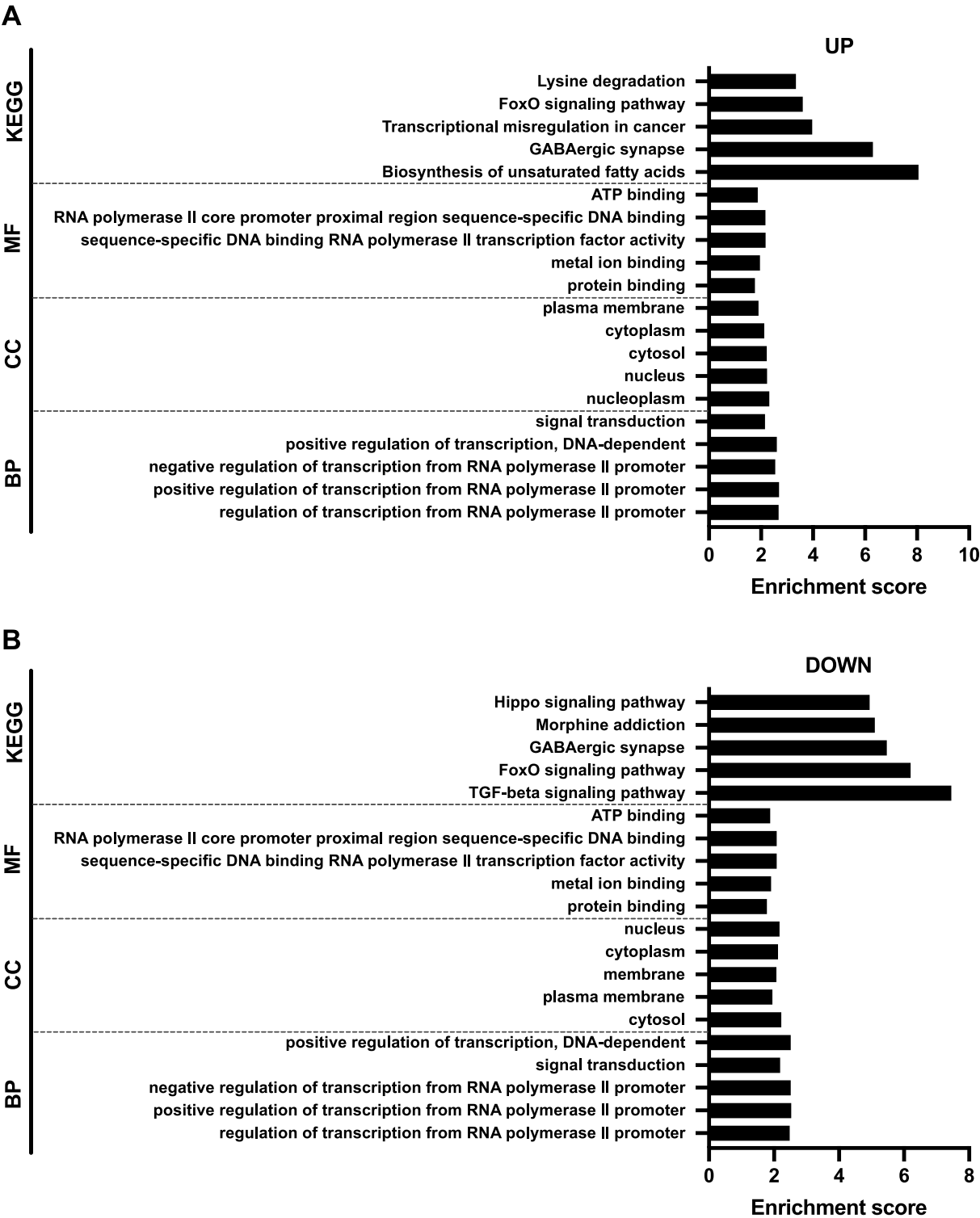


Fig. 4. PANTHER analysis performed a Gene Ontology and KEGG annotation of the identified DEGs. Abbreviations: DEG: differentially expressed gene; BP: biological process; CC: cellular component; MF: molecular function.

the timely identification of conditions. Our study introduces a straightforward and efficient method for isolating and accurately quantifying miRNAs in EVs from serum, confirming that miR-574-3p, miR-542-3p, and miR-200a-3p in serum EVs may serve as promising diagnostic markers for MASLD.

Exosomes, a subtype of EVs, play a crucial role in intercellular communication through the transfer of proteins and RNAs. miRNAs represent a highly conserved class of small, tissue-specific, non-coding

RNAs that regulate the expression of numerous functionally related genes. Hepatic-derived exosomal miRNAs have been shown to be closely associated with the development and progression of NAFLD through multiple mechanisms. The characterization of miRNAs in the exosomes suggests their potential as multifunctional biomarkers for NAFLD, therapeutic targets in clinical settings, and predictors of patient prognosis [14–16]. Ahmed M. Samy et al. isolated exosomes from plasma using ultracentrifugation and reported that exosomal miR-122 and

Table 2
The diagnostic value of serum exosomal miRNAs of MASLD and HC.

| miRNAs | AUC | Standard error | 95%CI | |
|---------------|-------|----------------|-------|-------|
| | | | Down | Up |
| miR-374a-5p | 0.877 | 0.088 | 0.703 | 1 |
| miR-510-3p | 0.790 | 0.110 | 0.575 | 1 |
| miR-574-3p | 0.809 | 0.102 | 0.608 | 1 |
| miR-100-5p | 0.778 | 0.113 | 0.557 | 0.999 |
| miR-542-3p | 0.833 | 0.095 | 0.647 | 1 |
| miR-6503-5p | 0.846 | 0.097 | 0.656 | 1 |
| miR-758-5p | 0.796 | 0.107 | 0.587 | 1 |
| miR-200a-3p | 0.802 | 0.111 | 0.584 | 1 |
| miR-1224-5p | 0.265 | 0.121 | 0.029 | 0.502 |
| miR-99b-5p | 0.167 | 0.097 | 0 | 0.356 |
| miR-3127-5p | 0.099 | 0.094 | 0 | 0.284 |
| miR-1185-2-3p | 0.173 | 0.098 | 0 | 0.366 |
| miR-548m | 0.247 | 0.119 | 0.014 | 0.48 |
| miR-3144-5p | 0.123 | 0.088 | 0 | 0.297 |
| miR-216b-5p | 0.037 | 0.042 | 0 | 0.12 |
| miR-873-3p | 0.160 | 0.098 | 0 | 0.352 |
| miR-378h | 0.235 | 0.114 | 0.011 | 0.458 |
| miR-608 | 0.222 | 0.115 | 0 | 0.448 |
| miR-1295a | 0.210 | 0.117 | 0 | 0.439 |

miR-128 were upregulated, while miR-200, miR-298, and miR-342 were downregulated in patients with nonalcoholic fatty liver and NASH compared to normal controls [15]. Similarly, Jeong-An Gim et al. isolated exosomes from serum using an exosome isolation kit and identified exosomal miRNAs correlated with inflammation, steatosis, ballooning, and nonalcoholic fatty liver disease activity scores (NAS) [16]. However, current techniques for isolating and quantifying exosomal miRNAs are often time-consuming, labor-intensive, and costly, limiting their practicality in clinical settings. In this study, we developed a novel and efficient approach for capturing and analyzing EVs using WGA-coupled magnetic beads combined with RT-qPCR. Our findings demonstrate that miR-574-3p, miR-542-3p, and miR-200a-3p in serum EVs hold

significant potential as promising diagnostic biomarkers for MASLD. In the investigation of the pathogenesis of MASLD, the traditional ‘second strike theory’ is progressively being superseded by the ‘multiple strike theory’ [17]. Within this framework, epigenetic factors, particularly miRNAs, emerge as essential components of epigenetic regulation. Research indicates that miRNAs are widely involved in fatty acid and cholesterol metabolism, glucose homeostasis, and insulin secretion [18]. Our study revealed significant differences in the levels of serum exosomal miR-574-3p, miR-542-3p, and miR-200a-3p between MASLD patients and healthy controls, as well as correlations with the severity of MASLD. Alessandra Tessitore et al. found miR-574-3p gradually increases as the severity of the disease during the transition NAFLD-NASH-HCC [19]. Zhou et al. found that miR-574-5p is significantly upregulated in serum exosomes and positively correlates with collagen deposition and alpha-SMA expression in liver tissues during fibrosis [20]. Li et al. discovered that miRNA-574-5p targets HOXC6 expression, thereby inhibiting lipid uptake in hepatocytes and mitigating non-alcoholic fatty liver disease [21]. Ji et al. demonstrated that miR-542-3p is significantly upregulated in hepatic fibrosis, promoting the activation of hepatic stellate cells, and facilitating the progression of

Table 3
The diagnostic value of serum exosomal miR-574-3p, miR-542-3p, miR-200a-3p of MASLD and HC.

| miRNA | AUC | Standard error | 95%CI | |
|---------------------------------------|-------|----------------|-------|-------|
| | | | Down | Up |
| miR-574-3p | 0.833 | 0.046 | 0.742 | 0.923 |
| miR-542-3p | 0.903 | 0.027 | 0.849 | 0.957 |
| miR-200a-3p | 0.825 | 0.070 | 0.686 | 0.962 |
| miR-574-3p + miR-542-3p | 0.943 | 0.017 | 0.910 | 0.976 |
| miR-574-3p + miR-200a-3p | 0.931 | 0.020 | 0.892 | 0.970 |
| miR-542-3p + miR-200a-3p | 0.919 | 0.032 | 0.857 | 0.982 |
| miR-574-3p + miR-542-3p + miR-200a-3p | 0.963 | 0.014 | 0.936 | 0.991 |

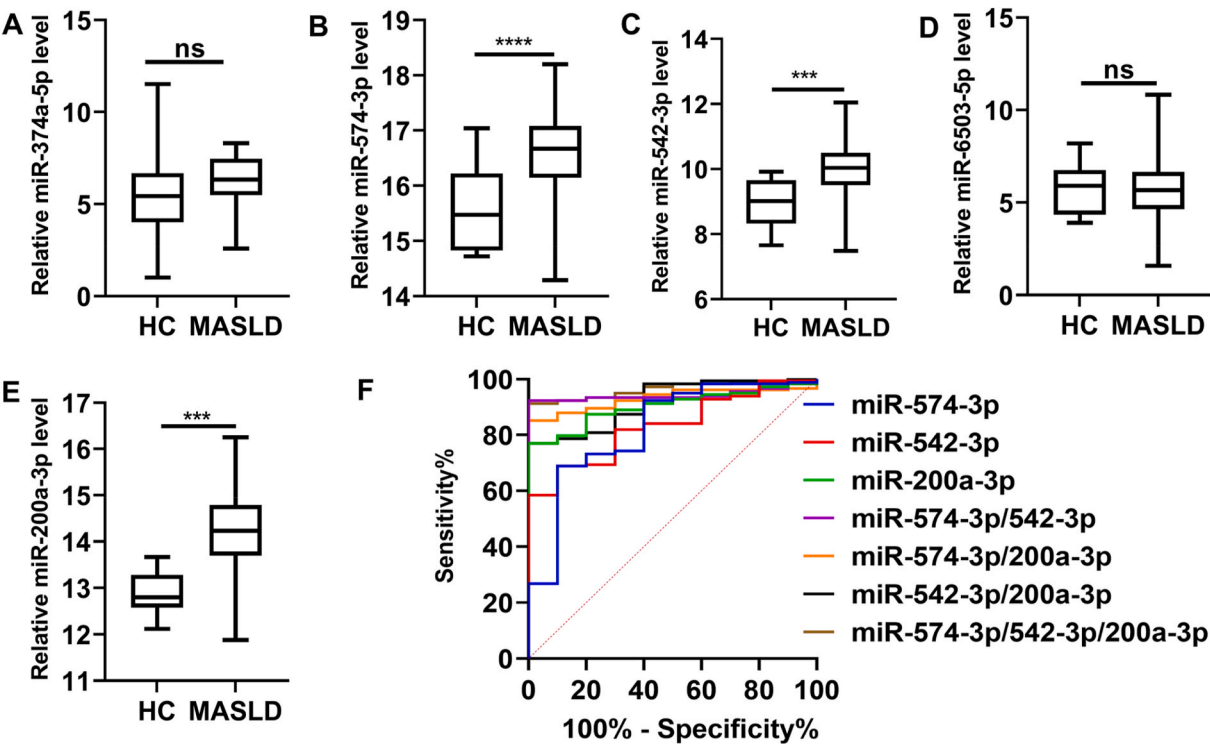


Fig. 5. miRNAs contained in exosomes used as markers for diagnosing MASLD. (A–E) Expression levels of miR-374a-5p, miR-6503-5p, miR-574-3p, miR-542-3p and miR-200a-3p in exosomes. (F) ROC curves analysis of miR-574-3p, miR-542-3p and miR-200a-3p in exosomes to distinguish MASLD from healthy control (HC). Data from three independent experiments (n = 3) were presented as mean ± SD. ns: $p \geq 0.05$; *** $p < 0.01$; **** $p < 0.001$.

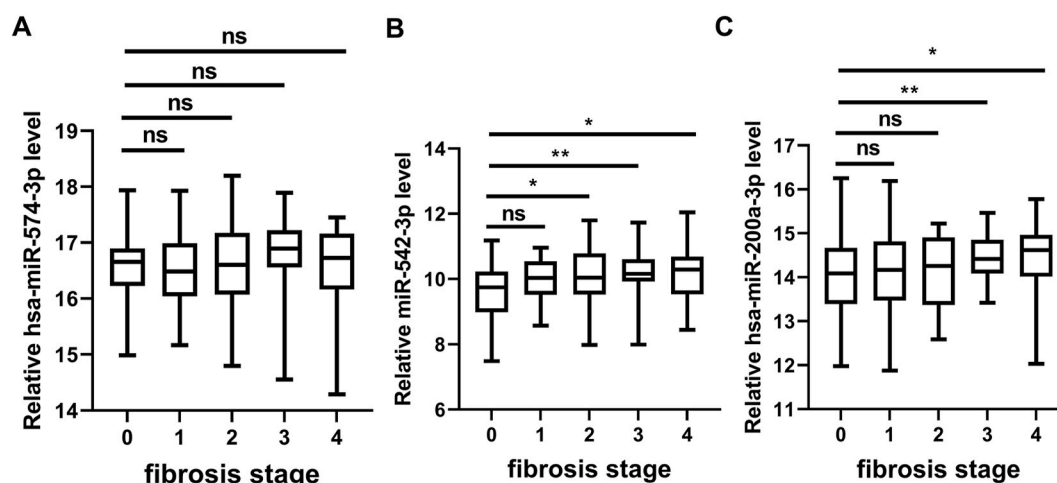


Fig. 6. Serum exosomal miR-542-3p and miR-200a-3p increased in advanced fibrosis. Data from three independent experiments were presented as mean \pm SD. ns: $p \geq 0.05$; * $p < 0.05$; ** $p < 0.01$.

fibrosis through the inhibition of BMP-7 [22]. Ye et al. reported that miR-200a-3p is significantly upregulated in fibrotic liver tissue, playing a pivotal role in liver fibrogenesis by repressing the expression of EGFR, STAT3, CTNNB1, and TP53 [23]. Liao et al. discovered that miR-200a-3p modulates hepatic stellate cell activation and potentially influences liver fibrosis pathogenesis through the inhibition of lncRNA Gpr137b-ps and CXCL14 [24]. Additionally, Huang et al. demonstrated that miR-200a-3p contributes to steatosis development by directly targeting the 3'-UTR of CYP3A4 [25]. These findings suggest that exosomal miR-574-3p, miR-542-3p, and miR-200a-3p may play significant roles in the occurrence and progression of MASLD.

This study has several limitations, especially the small sample size, despite the current data suggesting the potential of serum exosomal miR-574-3p, miR-542-3p, and miR-200a-3p in distinguishing MASLD. A more comprehensive study with a larger cohort is needed to validate these miRNAs as potential biomarkers for MASLD prior to clinical application. Additionally, the absence of follow-up data is another limitation; without it, we cannot determine whether serum exosomal miR-574-3p, miR-542-3p, and miR-200a-3p are associated with the progression of MASLD. In addition to MASLD, the liver may be affected by a variety of other diseases, such as viral hepatitis and drug-induced liver injury, which may also lead to changes in miRNAs of serum exosomes. The samples collected in this study also lack diversity. To utilize serum exosomal miR-574-3p, miR-542-3p, and miR-200a-3p as diagnostic biomarkers for MASLD, it is necessary to include a broader range of sample types to evaluate the accuracy and precision of these miRNAs as diagnostic biomarkers. Moreover, although previous studies have reported that miR-574-3p, miR-542-3p, and miR-200a-3p are involved in the occurrence and progression of MASLD [19–25], no research to date has elucidated the functions of exosomal miR-574-3p, miR-542-3p, and miR-200a-3p in intercellular communication during the pathogenesis of MASLD. Finally, although our methodology is relatively straightforward, RT-qPCR-based techniques still necessitate the use of Applied Biosystems Real-Time PCR Instruments. In future research endeavors, we aspire to devise a methodology for detecting serum exosomal miR-574-3p, miR-542-3p, and miR-200a-3p utilizing test strips in conjunction with WGA-coupled magnetic beads. This advancement would empower high-risk individuals to regularly monitor their risk of developing MASLD in the comfort of their homes or within the community through urine testing.

The pursuit of a non-invasive test for assessing MASLD risk has been ongoing for over 20 years. Our study indicates that serum exosomal miRNAs have the potential to serve as biomarkers for the presence of MASLD, potentially simplifying the process of direct examination and pathological testing for a definitive diagnosis. We validated the

expression levels of miR-574-3p, miR-542-3p, and miR-200a-3p in the exosomes of MASLD patients using RT-qPCR. The results showed that serum exosomal miRNAs were significantly elevated, indicating their potential as specific and sensitive biomarkers for diagnosing MASLD.

Data and materials availability

All data are available in the main text. Detailed raw data and information are provided by the corresponding author upon request.

Ethics approval and consent to participate

This study was approved by the Human Research Ethics Committee of the First Affiliated Hospital of Nanjing Medical University (2018-SR-069). All research was conducted in accordance with the Declarations of Helsinki and Istanbul.

Author contributions

Conceptualization: Yingyun Gong, Hongwei Liang, Hongwen Zhou.
Methodology: Moran Hu, Hai Huang and Min Xu.
Investigation: Moran Hu, Hai Huang, Meng Jia, Min Xu and Malin Chen.
Visualization: Moran Hu, Hai Huang, Min Xu, and Junxiang Wu.
Funding acquisition: Yingyun Gong and Hongwei Liang.
Resource: Shouyong Gu, Hongwen Zhou, Yingyun Gong.
Writing – original draft: Yingyun Gong.
Writing – review & editing: Yingyun Gong, Hongwei Liang, Hongwen Zhou.

Declaration of generative AI and AI-assisted technologies in the writing process

During the preparation of this work the authors used ChatGPT to improve language and readability. After using this tool, the authors reviewed and edited the content as needed and took full responsibility for the content of the publication. In addition, we declare no use of Generative AI or AI-assisted tools to create or alter images in submitted manuscripts.

Fundings

This work was supported by grants from the National Natural Science Foundation of China (No. 82270921 and No. 32170783), a fellowship from the China Postdoctoral Science Foundation (No. 2023M731407),

Basic research project of Jiangsu Science and Technology Office (No. BK20230075), and Jiangsu Provincial Medical Key Discipline (ZDXK202202).

Conflicts of interest

Authors declare that they have no competing interests.

Acknowledgement for support

We thank Nanjing Sirius Cell Engineering Co., Ltd. for technical support.

Appendix A. Supplementary data

Supplementary data to this article can be found online at <https://doi.org/10.1016/j.bj.2025.100838>.

References

- [1] Powell EE, Wong VW, Rinella M. Non-alcoholic fatty liver disease. *Lancet* 2021;397(10290):2212–24.
- [2] Wong VW, Ekstedt M, Wong GL, Hagström H. Changing epidemiology, global trends and implications for outcomes of NAFLD. *J Hepatol* 2023;79(3):842–52.
- [3] Zhou J, Zhou F, Wang W, Zhang XJ, Ji YX, Zhang P, et al. Epidemiological features of NAFLD from 1999 to 2018 in China. *Hepatology* 2020;71(5):1851–64.
- [4] Tilg H, Adolph TE, Dudek M, Knolle P. Non-alcoholic fatty liver disease: the interplay between metabolism, microbes and immunity. *Nat Metab* 2021;3(12):1596–607.
- [5] Di Mauro S, Scamporrino A, Filippello A, Di Pino A, Scicali R, Malaguarnera R, et al. Clinical and molecular biomarkers for diagnosis and staging of NAFLD. *Int J Mol Sci* 2021;22(21):11905.
- [6] Kalluri R, LeBleu VS. The biology, function, and biomedical applications of exosomes. *Science* 2020;367(6478):eaau6977.
- [7] O'Brien K, Breyne K, Ughetto S, Laurent LC, Breakefield XO. RNA delivery by extracellular vesicles in mammalian cells and its applications. *Nat Rev Mol Cell Biol* 2020;21(10):585–606.
- [8] Shang R, Lee S, Senavirathne G, Lai EC. microRNAs in action: biogenesis, function and regulation. *Nat Rev Genet* 2023;24(12):816–33.
- [9] Jafari N, Llevenen P, Denis GV. Exosomes as novel biomarkers in metabolic disease and obesity-related cancers. *Nat Rev Endocrinol* 2022;18(6):327–8.
- [10] Yang R, Zhang H, Chen S, Lou K, Zhou M, Zhang M, et al. Quantification of urinary podocyte-derived migrasomes for the diagnosis of kidney disease. *J Extracell Vesicles* 2024;13(6):e12460.
- [11] Huang H, Wan J, Ao X, Qu S, Jia M, Zhao K, et al. ECM1 and ANXA1 in urinary extracellular vesicles serve as biomarkers for breast cancer. *Front Oncol* 2024;14:1408492.
- [12] Li B, Hao K, Li M, Wang A, Tang H, Xu L, et al. Five miRNAs identified in fucosylated extracellular vesicles as non-invasive diagnostic signatures for hepatocellular carcinoma. *Cell Rep Med* 2024;5(9):101716.
- [13] Fracanzani AL, Valenti L, Bugianesi E, Andreoletti M, Colli A, Vanni E, et al. Risk of severe liver disease in nonalcoholic fatty liver disease with normal aminotransferase levels: a role for insulin resistance and diabetes. *Hepatology* 2008;48(3):792–8.
- [14] Zhang S, Liu YD, He ZD, Liu B, Linghu EQ. [Serum exosomal miRNAs profiling and functional study in patients with non-alcoholic fatty liver disease]. *Zhonghua Gan Zang Bing Za Zhi* 2021;29(10):987–94.
- [15] Samy AM, Kandeil MA, Sabry D, Abdel-Ghany AA, Mahmoud MO. Exosomal miR-122, miR-128, miR-200, miR-298, and miR-342 as novel diagnostic biomarkers in NAFL/NASH: impact of LPS/TLR-4/FoxO3 pathway. *Arch Pharm* 2024;357(4):e2300631.
- [16] Gim JA, Bang SM, Lee YS, Lee Y, Yim SY, Jung YK, et al. Evaluation of the severity of nonalcoholic fatty liver disease through analysis of serum exosomal miRNA expression. *PLoS One* 2021;16(8):e0255822.
- [17] Tilg H, Moschen AR. Evolution of inflammation in nonalcoholic fatty liver disease: the multiple parallel hits hypothesis. *Hepatology* 2010;52(5):1836–46.
- [18] Rottiers V, Najafi-Shoushtari SH, Kristo F, Gurumurthy S, Zhong L, Li Y, et al. MicroRNAs in metabolism and metabolic diseases. *Cold Spring Harb Symp Quant Biol* 2011;76:225–33.
- [19] Tessitore A, Ciciarelli G, Del Vecchio F, Gaggiano A, Verzella D, Fischietti M, et al. MicroRNA expression analysis in high fat diet-induced NAFLD-NASH-HCC progression: study on C57BL/6J mice. *BMC Cancer* 2016;16:3.
- [20] Zhou X, Liang Z, Qin S, Ruan X, Jiang H. Serum-derived miR-574-5p-containing exosomes contribute to liver fibrosis by activating hepatic stellate cells. *Mol Biol Rep* 2022;49(3):1945–54.
- [21] Li J, Song H, Chen Z, Yang Q, Yang Z, Yan C, et al. MicroRNA-574-5p targeting HOXC6 expression inhibits the hepatocyte lipid uptake to alleviate non-alcoholic fatty liver disease. *Exp Cell Res* 2023;428(1):113631.
- [22] Ji F, Wang K, Zhang Y, Mao XL, Huang Q, Wang J, et al. MiR-542-3p controls hepatic stellate cell activation and fibrosis via targeting BMP-7. *J Cell Biochem* 2019;120(3):4573–81.
- [23] Ye M, Wang S, Sun PL, Qie JB. Integrated MicroRNA expression profile reveals dysregulated miR-20a-5p and miR-200a-3p in liver fibrosis. *BioMed Res Int* 2021;2021:9583932.
- [24] Liao J, Zhang Z, Yuan Q, Liu Q, Kuang J, Fang Y, et al. A lncRNA Gpr137b-ps/miR-200a-3p/CXCL14 axis modulates hepatic stellate cell (HSC) activation. *Toxicol Lett* 2021;336:21–31.
- [25] Huang Z, Wang M, Liu L, Peng J, Guo C, Chen X, et al. Transcriptional repression of CYP3A4 by increased miR-200a-3p and miR-150-5p promotes steatosis *in vitro*. *Front Genet* 2019;10:484.